Trans. JSASS Aerospace Tech. Japan
Vol. 19, No. 5, pp. 794-801, 2021
DOI: 10.2322/tastj.19.794

Analysis of Motion Control for a Quadruped Ground-Gripping Robot for Minor Body Exploration on Uneven Terrain

By Warley F. R. RIBEIRO,[1)] Kentaro UNO,[1)] Kenji NAGAOKA,[2)] and Kazuya YOSHIDA[1)]

[1)]*Department of Aerospace Engineering, Tohoku University, Sendai, Japan*
[2)]*Department of Mechanical and Control Engineering, Kyushu Institute of Technology, Kitakyushu, Japan*

(Received July 12th, 2019)

The exploration of minor bodies, such as asteroids and comets using robotics is a necessary step for the study of the Solar System's evolutionary process. For such purpose, a multi-legged ground-gripping robot was proposed to perform precise locomotion towards specific places of interest. Moreover, stable locomotion is expected, since this robot has grippers capable of grasping the rocky and uneven terrain of the minor bodies, maintaining the attachment to the ground and preventing the flotation of the robot on the microgravity environment. Decreasing the forces induced on the grippers is essential to keep the stable locomotion in such environments and, in this paper, a gait control method is proposed to reduce accelerations and motion reactions on the robot, avoiding high reaction forces on the contact points with the ground. This method focuses on generating trajectories to be traveled by parts of the robot. A numerical simulation was developed to investigate the effectiveness of the proposed method in decreasing reactions on the robot during the motion of the robot on uneven terrains by comparing different trajectories' parameters.

Key Words: Ground-Gripping Robot, Robotic Exploration, Microgravity

Nomenclature

$\boldsymbol{a}$	:	spline curve coefficient
$\boldsymbol{c}$	:	non-linear velocity dependent term
D	:	damping coefficient
$\boldsymbol{F}$	:	force vector
$\boldsymbol{H}$	:	inertia matrix
$\boldsymbol{J}^T$	:	Jacobian transpose matrix
K	:	stiffness coefficient
k	:	control gain
n	:	number of legs
R	:	range
T	:	period
t	:	time
$\boldsymbol{x}$	:	position vector
β	:	duty ratio
$\boldsymbol{\tau}$	:	joint torque vector
$\boldsymbol{\phi}$	:	joint angle vector

Subscripts

0	:	initial
b	:	base
bm	:	base-manipulator coupling
c	:	contact point
d	:	derivative
des	:	desired
e	:	end-point
f	:	final
i	:	intermediary
m	:	manipulator (legs)
p	:	proportional
s	:	surface/gripper connection

1. Introduction

The use of robotics has been growing to explore different types of severe environments, such as disaster areas, regions affected by volcanic activities, and extraterrestrial bodies in outer space. All those locations have in common an unknown condition susceptible to dynamic changes, making exploration of the surface very challenging, which requires several types of equipment and suitable locomotion methods. For instance, Solar System minor bodies, such as asteroids and comets have been targeted for recent exploration missions, since they are believed to be either a sub-product or the forming pieces of current planets. Therefore, by studying asteroids and comets, we can understand the evolutionary process and formation of our Solar System.[1)] Furthermore, minor bodies may be a source of valuable resources, such as water and metals, which could be mined and processed to support further space exploration or to provide supplies for the Earth. In addition, technologies to change the course of near-Earth asteroids to protect our planet from dangerous impacts are recommended.[2)]

The surface of minor bodies is composed of many rocks of different sizes, making it a very jagged and irregular terrain. Gravity is more than a thousand times smaller than Earth's, causing the exploration of the surface to be even more challenging. Therefore, conventional locomotion methods, such as wheeled and tracked robots, which were extensively used for the past and current missions to Mars and the Moon, are not suitable for the exploration of environments under microgravity condition.

Innovative methods were proposed to accomplish the surface exploration of asteroids, such as Hayabusa and Hayabusa2 sample-return missions by the Japan Aerospace Exploration Agency (JAXA). Both spacecrafts were planned for a touch-and-go maneuver to collect samples, unnecessary to deal with continuous locomotion on the surface.[3,4)] Moreover, a jump-

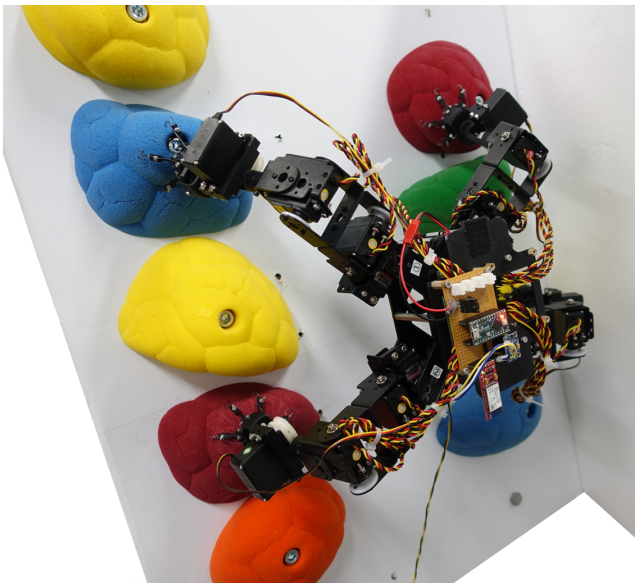

Fig. 1. Prototype of the ground-gripping robot.

ing robot called MINERVA was proposed to realize locomotion by taking advantage of the small gravity to jump over the minor body's surface.[5] During the Hayabusa2 mission, two MINERVA II-1 rovers successfully landed and hopped on the surface of the asteroid Ryugu, validating the jumping method as a potential means for locomotion.[6] However, uncontrollable bouncing after contact with the surface can make the robot move in an undesirable direction.

A multi-legged ground-gripping robot, as the one shown in Fig. 1, has been proposed to achieve stable and precise locomotion on the surface of asteroids.[7] This legged-robot features grippers at the end of each leg, allowing it to grasp onto the terrain and maintain contact with the surface, avoiding uncontrollable flotation. The motion towards a specific point of interest is expected to be achieved by accurately controlling the movement of the legs.

Since ground-gripping robots are expected to be a solution for stable and precise exploration of minor bodies, a few key technologies still have to be improved and developed. A reliable and robust gripper is necessary to guarantee a successful attachment to the ground. Moreover, some adaptability is needed to enable grasping rocks of different sizes. NASA/JPL developed a multispine gripper for a four-legged robot, to enable climbing on natural rocky terrains.[8,9] In our research group we developed a lightweight, passive gripper, capable of grasping rocks with fewer actuators.[10]

Additionally, high reaction forces could cause the gripper to slip from the grasped position, inducing an undesirable floating motion away from the surface. Control methods to reduce the gripper pulling action are also necessary for stable locomotion. Previously, we presented an algorithm based on reactionless control to improve the equilibrium of a planar two-legged walking robot in microgravity.[11] Our group also conducted studies on the gait analysis and path planning for legged-robots based on tumble stability.[12,13]

In this paper, we propose a control method to reduce the acceleration of a quadruped ground-gripping robot, that leads to more stable locomotion in a three-dimensional space under microgravity. First, the dynamic behavior of a legged robot is presented. We then introduce the control method by describing the gait sequence, the trajectories to be followed by the grippers and the base, and ultimately, the torque control of each joint. In addition, we define the walking simulation flow and the model of the robot. Finally, comparative simulation results are shown to validate the efficacy of the proposed method.

2. Dynamics of a Multi-Limbed Robot

The dynamic model description of a robot is essential to understanding the movement under any potential situation and predicting the future behavior of the system. Particularly in the absence of gravity, the inertial acceleration takes an important role in defining the stability and designing the gait pattern of a multi-limbed robot. The Equation of Motion (EoM) of a legged robot is necessary for the study of the locomotion, equilibrium, and control of a robot intended for the exploration of minor bodies.

2.1. Equation of motion

The EoM of a multi-legged robot can be written as the equation of a robot with multi-link manipulators connected to a free moving base, such as a free-flying manipulator, as shown in Eq. (1).[14] Here, we assume a robot with n legs walking on an environment with negligible gravitational force, and external forces acting only at the end of each limb.

$$\begin{bmatrix} \boldsymbol{H}_b & \boldsymbol{H}_{bm} \\ \boldsymbol{H}_{bm}^T & \boldsymbol{H}_m \end{bmatrix} \begin{bmatrix} \ddot{\boldsymbol{x}}_b \\ \ddot{\boldsymbol{\phi}} \end{bmatrix} + \begin{bmatrix} \boldsymbol{c}_b \\ \boldsymbol{c}_m \end{bmatrix} = \begin{bmatrix} \boldsymbol{F}_b \\ \boldsymbol{\tau} \end{bmatrix} + \begin{bmatrix} \boldsymbol{J}_b^T \\ \boldsymbol{J}_m^T \end{bmatrix} \boldsymbol{F}_e. \quad (1)$$

Here, $\boldsymbol{H}_b$, $\boldsymbol{H}_m$ and $\boldsymbol{H}_{bm}$ are the inertia matrices of the base, legs and base-legs coupling, respectively. Additionally, $\ddot{\boldsymbol{x}}_b$ is the base acceleration vector, $\ddot{\boldsymbol{\phi}}$ is the vector for the joint's angular acceleration, $\boldsymbol{\tau}$ is the vector for the input torque on the joints, $\boldsymbol{F}_b$ is the force vector acting on the robot's base and $\boldsymbol{F}_e$ is the vector with external reaction forces for all grippers. Additionally, $\boldsymbol{c}_b$ and $\boldsymbol{c}_m$ are the non-linear velocity dependent terms, while $\boldsymbol{J}_b^T$ and $\boldsymbol{J}_m^T$ are the Jacobian matrices for the base and legs, respectively.

2.2. Reaction forces

The locomotion of a legged robot is only possible due to driving forces from the interaction with the ground surface, which are mainly dominated by frictional phenomena. The active motion of the limb's end-points in contact with the terrain is, therefore, necessary for a robot to generate those driving forces. In the case of ground-gripping robots, a gripper-like mechanism guarantees the attachment to the surface without slipping by generating gripping forces that increase the friction.

When the planned movement is executed, reactions due to this motion are produced on other parts of the robot. The reactions due to the robot's own motion are inertial forces and affect the entire locomotion of the system, which need consideration for the analyses of the gripper attachment conditions.

Figure 2 illustrates the reaction forces acting on a quadruped robot. The first one, shown by red lines, is the reaction due to the executed motion, defined in this paper as motion reaction or internal inertial force; the other is the ground reaction force, or external force, which is the summation of the forces generated from the gripper and the internal inertial forces.

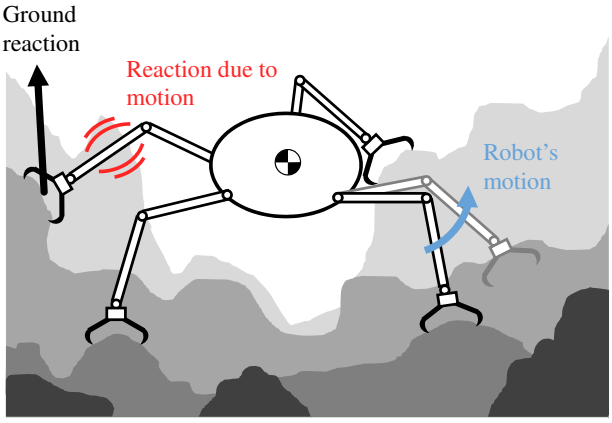

Fig. 2. Diagram of ground reaction force (external force) and reaction due to the robot's motion (internal inertial force).

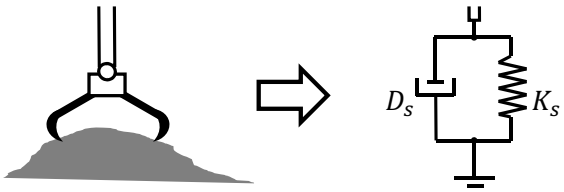

Fig. 3. Spring-damper model diagram of the external forces for the attachment of the gripper with the ground surface.

The ground reactions are the external forces obtained from each contact point of the ground-gripping robot with the surface, due to the friction between the terrain and the finger-tips of the grippers, and different models can describe this attachment.[15] In this paper, we consider a flexible connection between the leg end-point and the ground, based on a spring-damper model in all three linear directions, described by Eq. (2) and represented in Fig. 3. In this model, the equilibrium point for the external force $\boldsymbol{F}_e$ is the initial position $\boldsymbol{x}_c$ of the gripper when the attachment occurs. Small displacements are induced at each of the gripper positions $\boldsymbol{x}_e$ over the time t due to the motion reactions.

$$\boldsymbol{F}_e(t) = -K_s(\boldsymbol{x}_e(t) - \boldsymbol{x}_c) - D_s\dot{\boldsymbol{x}}_e(t), \tag{2}$$

where K_s and D_s are the stiffness and damping coefficients of the flexible attachment, respectively.

If the ground reaction forces exceed the threshold of the gripper maximum holding forces, the gripper detaches from the surface. Combining the modeling of the gripper with performance evaluation tests is an option to estimate the limit of holding forces.[10] However, the limit is highly dependent on gripping conditions and surface properties. Thus, we should consider conservative measures to define the maximum allowed force.

3. Control Method

The primary challenge when dealing with the stability of a ground-gripping robot on a microgravity environment is to prevent the detachment of the gripper from the previously grasped point, which would cause the robot to lose contact with the ground and float away from the surface. Therefore, reducing the pulling forces on the gripper is a necessary task for stable and continuous locomotion control. The method we present in this paper is based on the idea of decreasing the overall acceleration to reduce the motion reactions. The simplest way to lower the acceleration is decreasing the overall velocity of the robot, but there are more options to address this problem. We can plan a smooth trajectory for the robot to reduce motion acceleration. Furthermore, abrupt variations on the movement would not happen, resulting in fewer reactions due to the motion of the robot.

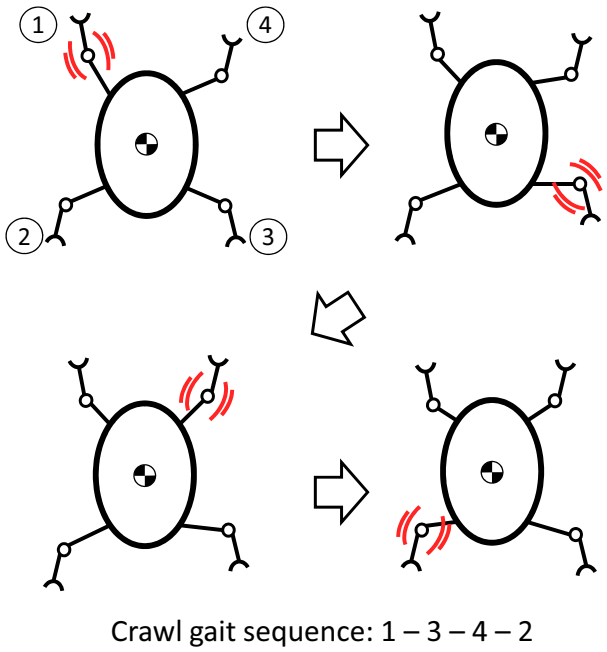

Fig. 4. Diagram to describe the gait sequence.

In this chapter, we describe the control of a quadruped robot to reduce the reaction motions. We start with the definition of the gait cycle pattern, by setting a periodic crawl gait to increase equilibrium. Next, we generate a smooth trajectory to be followed by the swing leg and the robot's base, aiming to lower the acceleration. Finally, we describe a PD torque control to drive the robot to achieve the planned motion.

3.1. Gait sequence

The gait of a robot determines the style of walking, defining the timing for each leg to move or stay in contact with the ground. Several walking patterns are observed in nature which serve as a source of inspiration for robot designers.[16] Among the possible motions, the periodic crawl gait is noted to be more stable since only one leg moves at a time, the reason why it was chosen in this paper to increase the equilibrium of the robot under microgravity. The swinging sequence is left-front leg, rear-right leg, front-right leg and rear-left leg, as shown in Fig. 4.

Some parameters are necessary to accurately define a gait, starting with the period T, which is the total time for one cycle of rising and lowering all limbs. Next, the duty ratio β is defined as the ratio of time for the supporting phase of one limb by the period T. For the crawl gait, the duty ratio is at least 0.75, where a higher value indicates a phase with four supporting legs. Finally, the range R is the distance traveled by the robot in one cycle.

3.2. Smooth trajectory

Smooth curves are often used in robotics to generate better trajectories for the locomotion of robots. One simple and well-known curve applied in path planning is the spline curve, which is defined by polynomial functions. The third-order spline curve, as expressed by Eq. (3), can be used to define the trajectory of the robot's base and swing limb during the motion, where $\boldsymbol{a}_0$, $\boldsymbol{a}_1$, $\boldsymbol{a}_2$ and $\boldsymbol{a}_3$ are the polynomial coefficients and t_0 is the initial time of the trajectory.

$$\boldsymbol{x}_e(t) = \boldsymbol{a}_0 + \boldsymbol{a}_1(t - t_0) + \boldsymbol{a}_2(t - t_0)^2 + \boldsymbol{a}_3(t - t_0)^3. \quad (3)$$

All four polynomial coefficients $\boldsymbol{a}_0$, $\boldsymbol{a}_1$, $\boldsymbol{a}_2$ and $\boldsymbol{a}_3$ can be calculated from Eq. (4), by setting initial and final positions, $\boldsymbol{x}_0$ and $\boldsymbol{x}_f$, initial and final velocities and initial and final times, t_0 and t_f.

$$\begin{aligned} \boldsymbol{a}_0 &= \boldsymbol{x}_0, \\ \boldsymbol{a}_1 &= \dot{\boldsymbol{x}}_0, \\ \boldsymbol{a}_2 &= \frac{-3(\boldsymbol{x}_0 - \boldsymbol{x}_f) - (t_f - t_0)(2\dot{\boldsymbol{x}}_0 + \dot{\boldsymbol{x}}_f)}{(t_f - t_0)^2}, \\ \boldsymbol{a}_3 &= \frac{2(\boldsymbol{x}_0 - \boldsymbol{x}_f) + (t_f - t_0)(\dot{\boldsymbol{x}}_0 + \dot{\boldsymbol{x}}_f)}{(t_f - t_0)^3}. \end{aligned} \quad (4)$$

The definition of spline parameters is based on achieving the desired location while trying to reduce motion reactions. Positions are selected based on the current grasping position and the next desired grasping position for the selected moving leg. The initial time is defined from the current time value that the robot starts the movement. The final time is calculated from the time parameters of the gait cycle, which is $(1-\beta)T$ for the swing time of a leg during a regular crawl gait or simply T for the base motion. Initial and final velocities are set to zero for a smooth variation of the gripper positions, from the static attachment state to the swing phase. In a practical situation, small velocities for the end-point can help to avoid the gripper scratching the ground while swinging, causing unnecessary external forces to act on the robot.

For the trajectory planning of the leg motion, we include an intermediary point between the current grasping position and the next desired grasping position for the selected moving leg. This intermediary point is needed to make the robot raise the gripper sufficiently to prevent collisions with the surface. The point is placed so that it is exactly in the middle of the distance from the current grasping point to the next desired grasping position, but with a height increment H in the z-direction, perpendicular to the ground surface. Two segments of splines curves connecting the three points make the designed trajectory. Hence, position, velocity, and time parameters of the intermediary point are also needed. As described, the intermediary position $\boldsymbol{x}_i$ is selected to be in half of the distance with a height increment. Time to reach the intermediary point t_i is also set as half of the total swing time. For the velocity at the intermediary point $\dot{\boldsymbol{x}}_i$, the choice is the average traveling velocity, calculated from total distance and swing time. Details of the trajectory with the intermediary point are shown in Fig. 5.

The differentiation of Eq. (3) leads to planned velocity and acceleration, which are also smooth polynomial curves. Therefore, the use of cubic spline curves is sufficient to obtain smooth curves until the acceleration level. Other smooth curves could also be applied to achieve the reduction of accelerations inducing motion reactions. In this paper, among different possible smooth curves, we selected cubic spline because of its simplicity to use and faster computation speed for the trajectory and its parameters by using only polynomial equations. Besides being simple, cubic spline curves can achieve the desired outcome we are aiming for, which is reducing velocity variations with respect to time.

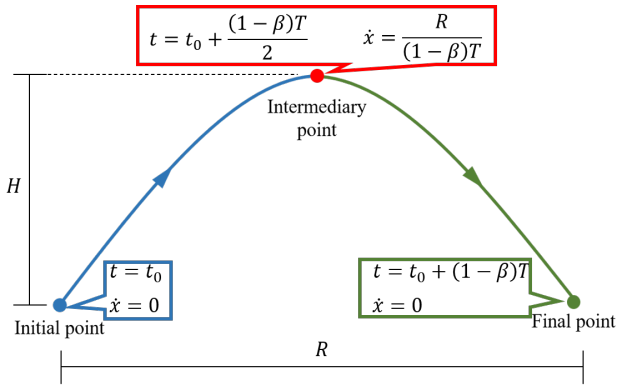

Fig. 5. Diagram of the spline trajectory of a swing leg with the addition of an intermediary point. Time t and velocity $\dot{\boldsymbol{x}}$ for each point are shown, together with traveling distance R and height H increment indication. Duty cycle β and walking cycle period T are parameters for the periodic crawl gait.

3.3. Torque control

The robot must be controlled to perform the planned gait pattern and follow the established smooth path, which aims to realize more stable locomotion. Usually, the movement of robots is achieved by using rotational motors to change the position of links that compose the legs. Different methods can be used to control those motors, but we assume a torque control in this paper.

From the positions calculated by splines, we can compute the necessary attitude of the robot for every step of the walking cycle. Inverse kinematics allows the calculation of the angular position of each joint from the assigned end-points and base positions, solving from the geometric point of view.

The input torque $\boldsymbol{\tau}$ for the joints is calculated by a proportional-derivative controller for the angular position $\boldsymbol{\phi}$ of the joints, compared with the desired positions $\boldsymbol{\phi}_{des}$ calculated from the inverse kinematics. Equation (5) shows the input torque calculation, where k_p and k_d are the proportional and derivative gains, respectively. Such gains must be tuned so that the robot can follow the planned trajectory accurately. Otherwise, the control is not adequate, and the robot might fail to grasp the desired position. Or even collide with the surface, inducing higher reaction forces.

$$\boldsymbol{\tau}(t) = k_p(\boldsymbol{\phi}_{des} - \boldsymbol{\phi}(t)) + k_d(\dot{\boldsymbol{\phi}}_{des} - \dot{\boldsymbol{\phi}}(t)). \quad (5)$$

4. Numerical Simulation

Numerical simulations enable the analysis of a robot's motion and dynamic behavior. From the mathematical model of the system, verifying the control methods and predicting robot's response can be investigated before real tests with prototypes.

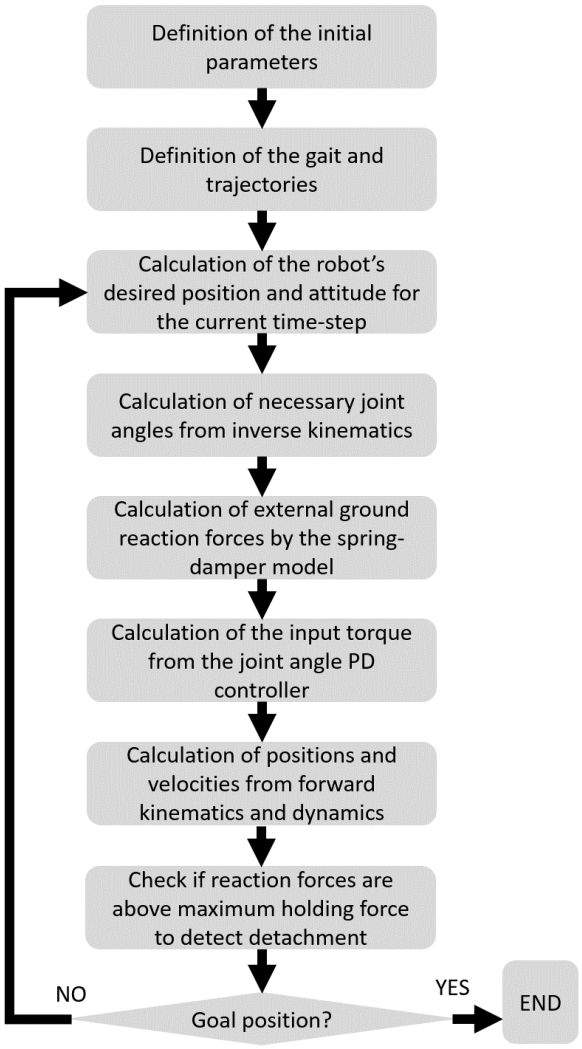

Fig. 6. Diagram of the numerical simulation flow.

We developed a simulation to verify the efficacy of the proposed control method, using the SpaceDyn Matlab toolbox for the dynamics calculation.[17] The simulation algorithm is shown in Fig. 6 and described below in details.

- Initial parameters definition: first, we set the parameters for the environment, such as the gravity value and the terrain shape and size. As well as defining of the model of the robot by determining its size, inertia parameters, links configuration, and the initial attitude.
- Gait determination: next, the parameters to generate the gait and the trajectories are defined and calculated, starting with the period and the gait sequence order. Distances to be traveled and the trajectory parameters are defined.
- Current step desired position calculation: starting the main loop of this algorithm, the desired position of the legs and the base are calculated from the current time value and the previously defined trajectory.
- Inverse kinematics: the necessary angles for the joints to achieve the desired attitude are calculated from the inverse kinematics, independently for each leg.
- External ground reaction forces: the forces acting on the end-point of each leg are calculated from a spring-damper model for the flexible connection between the supporting grippers and the terrain surface.
- Input torque control: the torque to be applied on each joint of the robot is calculated from a proportional-derivative controller for the desired angle joint, obtained from the inverse kinematics.
- Forward dynamics and kinematics: next, the accelerations, velocities, and positions of all links and end-points are calculated using the robot's equation of motion, for the given states of forces and input torques.
- Detachment detection: For each gripper, ground reaction forces are compared with the maximum holding force. The leg state changes to detached if the external force is greater than the maximum allowed force.
- Loop return check: Finally, the program checks if the robot reached the goal position to decide if it should end or return to the beginning of the loop to calculate the next step's desired position.

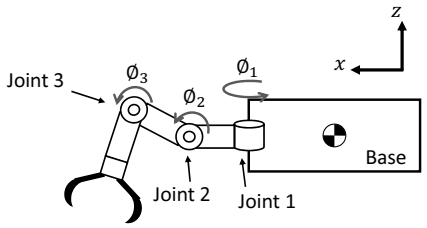

Fig. 7. Diagram of the arrangement of the links and joints of one leg of the robot used on the simulations.

Table 1. Summary of the robot parameters.

Items	Values	Unit
Base size	0.108×0.108	m^2
Link 1 length	0.0296	m
Link 2 length	0.0572	m
Link 3 length	0.1260	m
Total Mass	1.6	kg
Max. gripping force	5.9	N

4.1. Robot model

This simulation assumes a four-legged robot with grippers at the end of each limb, capable of attaching to the ground surface. Each leg has three links in a serial connection to the robot's base, providing the robot with twelve degrees of freedom. Three controllable rotational joints provide the required attitude and positional changes. Figure 7 shows the model of one leg of the quadruped robot with the arrangement of the links and joints. Table 1 exhibits the specific parameters for the size, mass, and gripping capacity of the modeled robot.

The maximum holding force was estimated based on pulling tests with a real gripper. Combining the results of the experiment with the model presented by Nagaoka et al., we observed that the gripper performs a minimum value of 5.9 N for the holding force considering all pulling directions.[10] We selected the minimum measured force as the gripper ' s holding force to assure that all possible detachments can be detected.

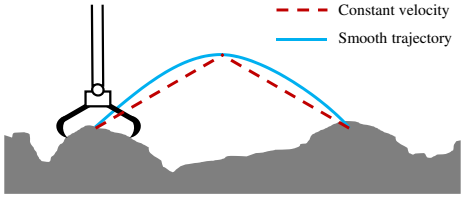

Fig. 8. Diagram of trajectories generation for both constant velocity and spline curves.

5. Simulation Results

The control method presented in this paper is verified by a comparative analysis between different trajectories for the motion of the quadruped robot on the developed simulation environment. The purpose is to evaluate which trajectory presents a better performance on the reduction of the reaction forces acting at each gripper attached to the ground. Two different comparisons are conducted to verify the influence of the time to travel and the shape of the trajectories.

First, we define the parameters for the simulations, and then an analysis of the ground reaction forces is conducted to compare the most effective parameters for the trajectory to obtain a gait with low reactions.

5.1. Simulation conditions

The environmental parameters are required to be set first. All simulations have the same conditions, i.e., a microgravity setting with a randomly generated uneven surface. The terrain based on the fractal surfaces theory has a roughness in the order of one centimeter, emulating a surface with small rocks on minor bodies. The gravity is determined as ten thousand times smaller than Earth's gravity. Stiffness and damping coefficients for the flexible connection between the ground and gripper are $K_s = 1000$ and $D_s = 1$, respectively.

The robot's initial position has its base center 8 cm above the ground surface. All the legs end-points are arranged diametrically opposed, making contact with the surface at a 19 cm distance from the center of gravity projection on the ground. The initial height of the grippers is decided accordingly to be precisely over the terrain.

For the gait control, the crawl gait with a duty ratio of $\beta = 0.75$ is considered for walking a distance of $R = 5$ cm traveled by each leg for one cycle, raising the gripper up to 3 cm from the starting positions. Finally, the proportional and derivative gains for the input torque control are $k_p = 3$ and $k_d = 0.02$, respectively. The gains, determined by the robot parameters and gravity field, were tuned based on a trial and error method such that the robot can follow different trajectories.

5.2. Comparison I: different shapes for trajectory

This first comparative study aims to verify the differences for trajectories of different shapes. For the generation of the trajectories, three points are considered: the initial position of the gripper, the next desired position obtained from the distance to be traveled, and an intermediary point, in the middle of the other two points, but 3 cm above the surface. Then, two paths connecting those three points are produced using either a straight line or a smooth spline curve. Figure 8 shows the concept for generating both trajectories. The period for one cycle was set to

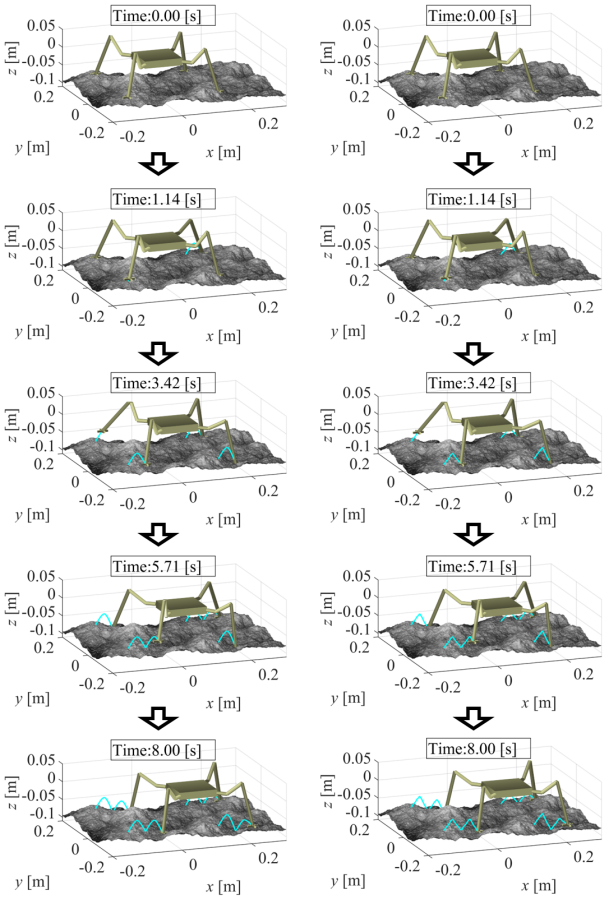

(a) Spline trajectory (b) Linear trajectory

Fig. 9. Motion sequence snapshots for the spline and linear trajectories.

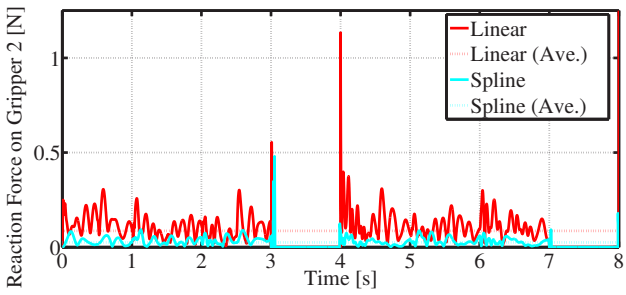

Fig. 10. Time history and average value of ground reaction forces for the smooth and linear trajectories simulation results.

$T = 4$ s, leading to a swing time of 1 s for each leg with a duty ratio of $\beta = 0.75$.

The outcome for the smooth and linear trajectories is shown in Fig. 9, which display the motion sequence of the robot for two walking cycles. The result for the ground reaction forces acting on the tip of leg number two is shown in Fig. 10, where the red line is for the linear trajectory, and the blue line shows the reaction forces when the smooth path is used. The mean value of the external force for both methods is also present on the same graph with dotted lines. Similar behavior is found for all the remaining legs.

By comparing the motion sequences for both simulations, little difference was observed and, in both cases, the robot was able to reach the goal position, 10 cm ahead of the initial point. However, looking into the graph for external reaction forces,

the effectiveness of the proposed trajectory with smooth spline curves in reducing reaction forces is clear. The comparison of the average values of the forces acting on the gripper number two, as defined in Fig. 4, shows a reduction of 66.4%, from 0.084 N to 0.028 N, by using the smooth trajectory instead of the linear trajectory with constant velocities. Considering that the detachment of the gripper occurs when the external force reaches a specific value, the maximum force value is also evaluated. A reduction of 61.6% is observed for these simulations since the maximum force for the linear trajectory was 1.25 N and 0.48 N for the spline curve. Because no abrupt changes are observed on the robot by implementing the spline-based trajectory, the internal reactions are lower than the constant velocity based trajectory, where sudden variations in the velocity cause undesired reactions.

From those results, we understand that a path with smooth characteristics induces fewer motion reactions on the robot, providing a movement with lower reaction forces. This confirms the applicability of the proposed method, increasing the stability and preventing detachment of the grippers from the surface.

5.3. Comparison II: different velocities for trajectory

The second analysis focuses on differences in the traveling speeds of a swing leg. The new trajectories consider the same path, generated from the spline curve described for the first comparison, but with a change in the period of the walking cycle. This change in time results in a different velocity since the traveled distance is the same. We consider two simulations of four cycles of motion where the goal is 20 cm ahead of the initial position, one with a period of $T = 2$ s for low-velocity, and the other with $T = 1$ s for high-velocity. In other words, since four cycles are required, the first simulation has a traveling velocity of 2.5 cm/s (low-velocity), while the second has a speed of 5 cm/s (high-velocity).

The motion sequence for both cases of low-velocity and high-velocity are presented in Fig. 11 (a) and Fig. 11 (b), respectively. Ground reaction forces acting on the third gripper are shown in the graph on Fig. 12, where the red line shows the reactions for low-velocity motion, and the blue line shows the reaction forces for high-velocity. The average value of the external force is also presented by dotted lines for both methods.

Considering the evaluation of the motion of the robot for the low-velocity case, a stable motion until the robot reaches the goal is observed. However, flotation of the robot is indicated in Fig. 11 (b) for the high-velocity locomotion. This second simulation presents a case where the external reaction forces are too high and induce the detachment of the gripper. This detachment can be confirmed from the reaction force graph, where the peak ground reaction force is observed as 7.54 N at 1.5 s, for high-velocity, which is higher than the pulling force limit of 5.9 N. All grippers presented a similar behavior with high external forces, gradually detaching the robot from the ground and, due to the absence of forces to push the robot to the surface, provoking the flotation of the ground-gripping robot. Such high reactions do not appear for low-velocity locomotion since the maximum external force is 2.89 N.

These results emphasize the necessity to decrease the motion reactions of the robot to prevent the detachment of the grippers. Such instability results in the slip of the grippers induced by

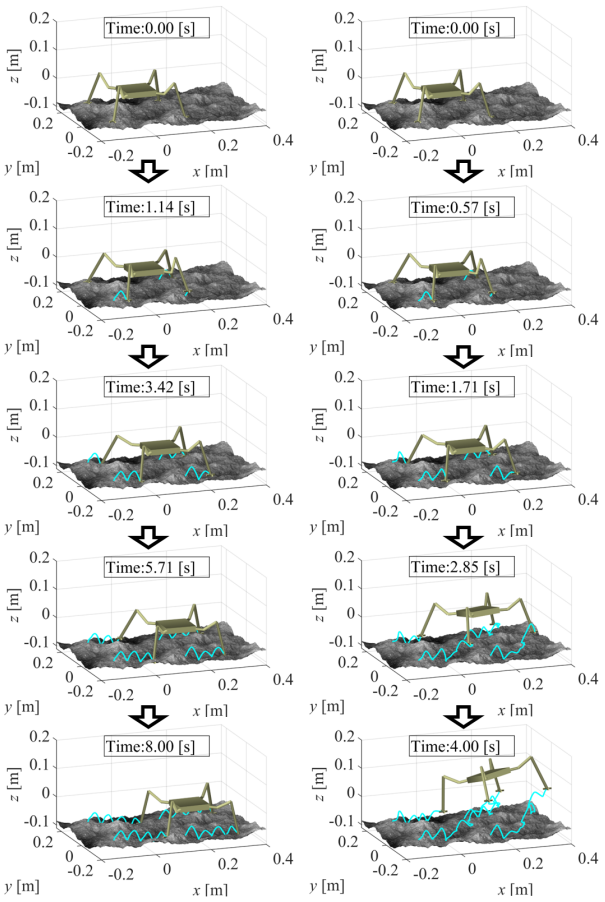

(a) Low-velocity (b) High-velocity

Fig. 11. Motion sequence snapshots for the low-velocity and high-velocity motions.

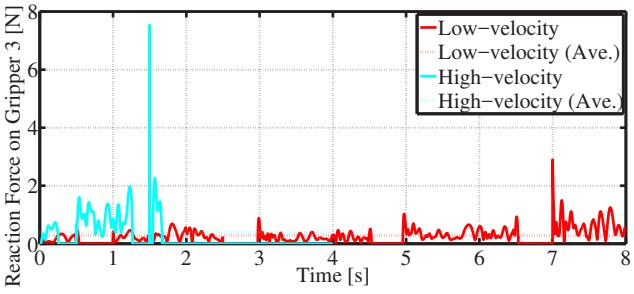

Fig. 12. Time history and average value of ground reaction forces for the low-velocity and high-velocity simulation results.

high accelerations. High-velocity motions are one of the major causes of high accelerations in the robot's movement. Therefore, moving in low-velocity is necessary for the stability of a robot under microgravity environments.

Planning the optimal velocity of the robot is an essential step to secure the stable motion of a ground-gripping robot while keeping the time efficiency of the mission. Numerical simulations are useful to test if the designed locomotion is safe or not, given that we have a reliable estimation of terrain shape, contact parameters, robot modeling, and others.

6. Conclusion

In this paper, we presented a method to reduce the motion reactions of a ground-gripping legged-robot for exploration on minor bodies with uneven terrains, by using a control that generates a smooth path for the swing limb and the base. In order to avoid the slip of the gripper and keep the stability during motion, a spline trajectory was proposed to reduce the acceleration of the robot, decreasing the motion reactions. A numerical simulation was conducted based on ground-gripping robot dynamics to compare different motions of the robot based on the proposed method. The results show a significant reduction of the forces acting on the point of contact between the robot and the surface for the smooth trajectories with low-velocity.

Acknowledgments

We express our special thanks to Ms. Victoria Keo for her considerable effort on developing and adapting the proposed algorithm for the uneven terrain case.

References

1) Leinhardt, Z. M. and Stewart, S. T.: Collisions Between Gravity-Dominated Bodies. I. Outcome Regimes and Scaling Laws, *The Astrophysical Journal*, **745** (2012), pp. 79–105.
2) Sanchez, J. P. and Garcia-Yarnoz, D.: Asteroid Retrieval Missions Enabled by Invariant Manifold Dynamics, *Acta Astronautica*, **127** (2016), pp. 667–677.
3) Kubota, T., Otsuki, M., and Hashimoto, T.: Touchdown Dynamics for Sample Collection in Hayabusa Mission, Proceedings of the 2008 IEEE International Conference on Robotics and Automation, Pasadena, CA, USA, pp. 158–163, 2008.
4) Watanabe, S., et al.: Hayabusa2 Arrives at the Carbonaceous Asteroid 162173 Ryugu – A Spinning Top-shaped Rubble Pile, *Science*, (2019), eaav8032.
5) Yoshimitsu, T., Kubota, T., Nakatani, I., Adachi, T., and Saito, H.: Micro-hopping Robot for Asteroid Exploration, *Acta Astronautica*, **52** (2003), pp. 441–446.
6) Japan Aerospace Exploration Agency: MINERVA-II1: Successful image capture, landing on Ryugu and hop!, 2018, http://www.hayabusa2.jaxa.jp/en/topics/20180922e/, (accessed March 11, 2019).
7) Yoshida, K., Maruki, T., and Yano, H.: A Novel Strategy for Asteroid Exploration with a Surface Robot, Proceedings of the 34th COSPAR Scientific Assembly, Houston, TX, USA, pp. 281–286, 2002.
8) Parness, A., Frost, M., Thatte, N., King, J. P., Witkoe, K., Nevarez, M., Garrett, M., Aghazarian, H., and Kennedy, B.: Gravity-independent Rock-climbing Robot and a Sample Acquisition Tool with Microspine Grippers, *Journal of Field Robotics*, **30** (2013), pp. 897–915.
9) Parness, A., Abcouwer, N., Fuller, C., Wiltsie, N., Nash, J., and Kennedy, B.: LEMUR 3: A Limbed Climbing Robot for Extreme Terrain Mobility in Space, Proceedings of the 2017 IEEE International Conference on Robotics and Automation, Singapore, Singapore, pp. 5467–5473, 2017.
10) Nagaoka, K., Minote, H., Maruya, K., Shirai, Y., Yoshida, K., Hakamada, T., Sawada, H., and Kubota, T.: Passive Spine Gripper for Free-Climbing Robot in Extreme Terrain, *IEEE Robotics and Automation Letters*, **3** (2018), pp. 1765–1770.
11) Yuguchi, Y., Ribeiro, W. F. R., Nagaoka, K., and Yoshida, K.: Analysis on Motion Control Based on Reaction Null Space for Ground Grip Robot on an Asteroid, *Trans. JSASS Aerospace Technology Japan*, **14**, ists30 (2016), pp. Pk_125–Pk_130.
12) Shirai, Y., Minote, H., Nagaoka, K., and Yoshida, K.: Gait Analysis of a Free-Climbing Robot on Sloped Terrain for Lunar and Planetary Exploration, Proceedings of the 14th International Symposium on Artificial Intelligence, Robotics and Automation in Space, Madrid, Spain, #2a-2, 2018.
13) Uno, K., Ribeiro, W. F. R., Jones, W., Shirai, Y., Minote, H., Nagaoka, K., and Yoshida, K.: Gait Planning for a Free-Climbing Robot Based on Tumble Stability, Proceedings of the 2019 IEEE/SICE International Symposium on System Integration, Paris, France, pp. 289-294, 2019.
14) Yoshida, K.: A General Formulation for Under-Actuated Manipulators, Proceedings of the 1997 IEEE/RSJ International Conference on Intelligent Robot and Systems, Grenoble, France, Vol. 3, pp. 1651–1657, 1997.
15) Ehsaniseresht, A. and Moghaddam, M. M.: A New Ground Contact Model for the Simulation of Bipeds' Walking, Running and Jumping, Proceedings of the 2015 3rd RSI International Conference on Robotics and Mechatronics, Tehran, Iran, pp. 535-538, 2015.
16) Hirose, S., Fukuda, Y., Yoneda, K., Nagakubo, A., Tsukagoshi, H., Arikawa, K., Endo, G., Doi, T., and Hodoshima, R.: Quadruped Walking Robots at Tokyo Institute of Technology, *IEEE Robotics & Automation Magazine*, **16** (2009), pp. 104–114.
17) Yoshida, K.: The SpaceDyn: a MATLAB Toolbox for Space and Mobile Robots, Proceedings of the 1999 IEEE/RSJ International Conference on Intelligent Robots and Systems, Kyongju, South Korea, Vol. 3, pp. 1633–1638, 1999.